A Vortex-Lattice Method for Calculating Longitudinal Dynamic Stability Derivatives of Oscillating Delta Wings

D. Levin*
NASA Ames Research Center, Moffett Field, California

A nonsteady vortex-lattice method is introduced for predicting the dynamic stability derivatives of a delta wing undergoing an oscillatory motion. The analysis is applied to several types of small oscillations in pitch. The angle of attack varied between ±1 deg, with the mean held at 0 deg when the flow was assumed to be attached and between ±1 deg and the mean held at 15 deg when both leading-edge separation and wake rollup were included. The computed results for damping in pitch are compared with several other methods and with experiments, and are found to be consistent and in good agreement.

Nomenclature

A_{ij} = influence coefficient
a_p = panel chord
B_{ij} = influence coefficient
C = wing chord
C_D = drag coefficient
C_{ij} = influence coefficient
C_L = lift coefficient
C_M = moment coefficient
C_{M_q} = moment coefficient due to pitch velocity
C_{M_θ} = m_θ – moment coefficient due to θ
$C_{M_{\dot\theta}}$ = $m_{\dot\theta}$ – moment coefficient due to $\dot\theta$
C_p = $p-p_\infty/\frac{1}{2}\rho U^2)$, pressure coefficient
$F(\ )$ = function
h = panel vertical distance
M = moment
P = panel
p,q,r = angular velocity about x,y,z axes, respectively
s = wing area
t = time
U = freestream velocity
u,v,w = induced velocity in the x,y,z directions, respectively
x,y,z = wing coordinates
α = angle of attack
Γ = circulation
Γ_f = wing-bound circulation
Γ_s = separated wake circulation
Γ_w = trailing-edge wake circulation
θ = oscillation angle
$\dot\theta$ = $d\theta/dt$, time derivative of oscillation angle
ν = reduced frequency
ρ = density
ϕ = potential
ω = frequency

Introduction

THE calculation of the dynamic stability derivatives has always been an essential as well as a difficult part of the aerodynamic design of aircraft. Today this task has become even more cumbersome. The achievement of high subsonic and supersonic flight speeds involved changes in the typical aerodynamic configurations, for example, highly swept and low-aspect-ratio wings, wing body, wing canard, or wing nacelle interactions, and long nose shapes. These changes can cause serious stability problems. The demand for higher maneuverability throughout the "nonlinear" angle of attack range, including poststall effects, has increased the difficulty in obtaining the stability derivatives by either theoretical estimation or experimental measurements. The effects of nonlinear forces and moments, flow separation, components interference, and the cross coupling between longitudinal and lateral motion are being investigated, but more theoretical as well as experimental efforts need to be invested.

Early works on dynamic stability are summarized by Thomas[1] and Ellison and Hoak,[2] whose investigations also serve to establish the significant derivatives the designer has to obtain. The work by Schneider[3] summarizes, to a great extent, the experimental and theoretical efforts that have been carried out in recent years. In the subsonic region, the assumption of potential flow leads to an integral equation for the downwash on the wing. Two general approaches are being used to solve this equation. The kernel-function method can solve the integral equation directly, obtaining a continuous distribution of singularity elements on the wing. This method underwent several stages of development, from early works, e.g., Ref. 4, which adapted the method for slow oscillations, to current works by Lehrian and Garner[5] and Morino,[6] to mention just a few, with which general oscillations can be solved. These approaches are limited to simple configurations—small harmonic oscillations about a linear mean angle of attack; they are being used to predict aerodynamic response to flutter and gust.

The other approach is based on the finite element concept. This method transforms the integral equation into a set of linear algebraic equations. In this manner complicated geometries can be handled, as reported in the works of Kalman et al.[7] and Dusto and Epton.[8] These works still use small oscillation about a mean linear flow condition, thus limiting the solution to small harmonic oscillations. These works are also limited to angles of attack in the linear range, since neither leading-edge separation nor wake rollup is allowed.

A study of unsteady aerodynamic loads with allowance for leading-edge separation and wake rollup was reported by Atta et al.,[9] Kandil et al.,[10] and Kandil.[11] A panel system was utilized to simulate leading-edge separation in steady-state flow. They performed calculations for several nonsteady motions such as rolling and pitch oscillation. However, their method is based on quasisteady steps, wherein the steady iterative calculations are performed at each step, limiting the validity of the method to slow aerodynamic processes.

Presented as Paper 81-1876 at the AIAA Atmospheric Flight Mechanics Conference, Albuquerque, N. Mex., Aug. 19-21, 1981; submitted Oct. 30, 1981; revision received March 23, 1983.

*NRC Associate. Member AIAA.

The time-dependent analysis of a wing with the wake-shedding procedure provides calculations for the nonsteady unrestricted motion, allowing for leading-edge separation and wake rollup. Such a method was developed by Djojodihardjo and Widnall[12] and Belotserkovskii[13]; it was also used by Summa[14] to solve complex wake shapes behind wings and behind helicopter rotors. The method of Refs. 12 and 14 did not have the leading-edge separation feature, and the works of Belotserkovskii do not furnish enough information. The present method utilizes the idea of time-dependent wake shedding. The present paneling system is similar to that of Rom et al.,[15] which simulates successfully the leading-edge separation and wake rollup in steady flow. Their method was extended to impulsively started wings by Levin and Katz[16] to provide predictions for both the transient and steady-state cases. This latter method is used to predict the dynamic stability derivatives of a delta wing in subsonic flow.

Method

The present method models the nonsteady flow over a thin delta wing in the low subsonic or incompressible region. The basic assumption common to all vortex-lattice methods is that for irrotational homogeneous flows such as this, a potential solution can be applied provided the viscous effects are properly modeled. The information needed for such modeling is supplied by experiments, flow visualization, or viscous flow calculations; it serves as an input to the potential solution.

The velocity potential assumption enables the continuity equation to be written as Laplace's equation

$$\nabla^2\phi = 0 \tag{1}$$

with the following boundary conditions: 1) there is no flow through the wing surface, and 2) the induced velocity of the wing decays far from the wing, everywhere except near the wake. Another condition that has to be satisfied by the solution is Kelvin's theorem, namely, that there is no change in the net circulation in the field at any time step, or

$$d\Gamma/dt = 0 \tag{2}$$

The Vortex-Lattice Model

A method for solving Laplace's equation with the boundary conditions mentioned above was proposed by Katz and Weihs,[17] and a model reflecting this approach was introduced in Ref. 16 (e.g., Fig. 1). The model consists of a first-order panel system having a constant bound vortex in each quarter chord of a rectangular cell. A collocation point is located in each cell at the three-quarter point of the centerline. The triangular panels are constructed similar to the way suggested in Ref. 15. The bound vortex lies between the quarter point of the root chord and the tip, and the collocation point is in the meridian intersection with the line going from the three-quarter point of the root chord to the tip. This panel system provided good predictions for the steady-state cases. The separated vortex strength Γ_{s_i} could be adjusted from zero to the full magnitude of the bound vortex Γ_{f_i}, in order to simulate various leading-edge radii; however, in the current use, sharp leading edges were assumed, and fully separated flow was used at high angles of attack.

The vortex-lattice model is already fulfilling the differential equation (1) and the boundary condition 2 (above), since the induced velocity of vortex filaments decays with distance. Equation (2) is satisfied by constructing the vortices in a closed configuration, as shown in Fig. 1, so that the net circulation in each time step is zero. The boundary condition 1 is being satisfied at all the collocation points. Defining all the velocity components at these points, generated by the wing's motion, the bound vortices, and the wake, leads to a system of linear algebraic equations. The solution of the latter provides the vortex's strength distribution on the wing. The preceding mathematical formulation becomes

$$-[U-ry_i]\sin(\alpha_i) - qx_i - py_i + \frac{\partial hi}{\partial t} = [A_{ij}]\begin{bmatrix}\Gamma_{f_1}\\ \vdots \\ \Gamma_{f_i}\\ \vdots \\ \Gamma_{f_n}\end{bmatrix} + [B_{ij}]\begin{bmatrix}\Gamma_{w_1}\\ \vdots \\ \Gamma_{w_i}\\ \vdots \\ \Gamma_{w_m}\end{bmatrix} + [C_{ij}]\begin{bmatrix}\Gamma_{s_1}\\ \vdots \\ \Gamma_{s_i}\\ \vdots \\ \Gamma_{s_\ell}\end{bmatrix} \tag{3}$$

Here p,q,r is the rotational motion around the x,y,z axes; correspondingly, $U(t)$ is the momentary far-field velocity, and α_i the panel angle of attack. The heaving motion of the panel relative to the x,y,z axes is $h_i(t)$, and its effect on the downwash is the $\partial h_i/\partial t$ term in Eq. (3). The first term on the right, A_{ij}, stands for all the influence coefficients resulting from the Biot-Savart bound vortex influence calculations.[18] The second and third terms, B_{ij} and C_{ij}, represent the influence coefficients of the trailing-edge wake Γ_{w_i} and leading-edge separated elements Γ_{s_i}, the strength of which is known from previous time steps. Equation (3) is derived for all n panels on their collocation points, resulting in n equations with n unknown Γ_{f_i} at each time interval. If the wing shape is not varying during flight (flap motion, ailerons, etc.), the coefficients A_{ij} are constant and their calculation is performed only once. The calculation efforts of B_{ij} and C_{ij} increase with time as the number of wake elements grows. This must be performed at each time interval since wake rollup changes the geometry involved in its induced-velocity calculations.

Calculational Procedure

To demonstrate the calculational procedure it is assumed that at $t=0$ the wing was suddenly set into motion. The first calculation takes place at $t=t_0$ (shown in Fig. 1b), and the spanwise wake vortex is placed in the midinterval traveled ($\frac{1}{2}U\Delta t$). For the linear (not separated) transient calculation there is no direct coupling between the panel length a_p and the time step, but for more precise accuracy the nondimensional time step should be smaller than 0.2 ($\Delta U/c<0.2$). For separated flow, however, it is recommended that the time steps and the panel lengths be of the same order of magnitude ($\Delta U/a_p=1$) to prevent the separated wake elements from being too close to the wing collocation points.

After the first time step the momentary position and angular motion of the wing are known and the geometrical boundary condition for the downwash [left-hand side of Eq. (3)] is determined. Then the influence coefficients A_{ij} are calculated while $B_{ij}=C_{ij}=0$ for the first time step, since there are no free wake elements shed as yet. At this point the bound vorticity strength Γ_{f_i} is solved and the wake rollup step is performed by moving the wake points shed at $t=t_0$. The downwash at each vortex edge location $(u,v,w)_i$ is calculated by Eq. (4) which is similar to the right-hand side of Eq. (3), but here $A_{w_{ij}}$, $B_{w_{ij}}$, and $C_{w_{ij}}$ are the influence coefficients relative to those vortex edges.

$$(u,v,w)_i = [A_{w_{ij}}]\begin{bmatrix}\Gamma_{f_1}\\ \vdots \\ \Gamma_{f_i}\\ \vdots \\ \Gamma_{f_n}\end{bmatrix} + [B_{w_{ij}}]\begin{bmatrix}\Gamma_{w_1}\\ \vdots \\ \Gamma_{w_i}\\ \vdots \\ \Gamma_{w_m}\end{bmatrix} + [C_{w_{ij}}]\begin{bmatrix}\Gamma_{s_1}\\ \vdots \\ \Gamma_{s_i}\\ \vdots \\ \Gamma_{s_\ell}\end{bmatrix} \tag{4}$$

Here the numbers of the separated wake, trailing-edge wake, and wing-vortex elements are ℓ, m, and n, respectively. The motion of the vortex-tip point $(\Delta x, \Delta y, \Delta z)_i$ is then calculated by the use of Eq. (5)

$$(\Delta x, \Delta y, \Delta z)_i = (u, v, w)_i \Delta t \tag{5}$$

To conclude the calculational procedure for a given time step, the forces acting on the foil are determined by applying the nonsteady Bernoulli equation as derived in Ref. 19. That is,

$$\frac{P_\infty - P}{\rho} = (U - ry)\frac{\partial \phi}{\partial x} + \frac{\partial \phi}{\partial t} + \frac{1}{2}\left[\left(\frac{\partial \phi}{\partial x}\right)^2 + \left(\frac{\partial \phi}{\partial y}\right)^2 + \left(\frac{\partial \phi}{\partial z}\right)^2\right] \tag{6}$$

By integrating the pressure along a given panel with length of $\Delta x_i = x_{i+1} - x_i$ and by neglecting smaller terms $[U(t) \gg (\partial\phi/\partial x), (\partial\phi/\partial y), (\partial\phi/\partial z)]$ and assuming $r = 0$ for the present calculation, the following expression for the normal force per unit width on the panel can be derived:

$$\Delta F_i = 2\rho\left(U\int_{x_i}^{x_{i+1}} \frac{\partial \phi}{\partial x}\,dx + \int_{x_i}^{x_{i+1}} \frac{\partial}{\partial t}\int_0^x \frac{\partial \phi}{\partial x}\,dx\,dx\right)$$

$$= \rho\left\{U\Gamma_{f_i} + \frac{\partial}{\partial t}\left[\left(\sum_{k=1}^{i}\Gamma_{f_k} + \sum_{k=1}^{i+1}\Gamma_{f_k}\right)\frac{\Delta x}{2}\right]\right\} \tag{7}$$

Here the summation

$$\sum_{k=1}^{i}\Gamma_{f_k}$$

is performed along the chord line only, starting at the leading-edge panel ahead of the panel for which the normal force ΔF_i is to be calculated. The momentary lift and drag coefficient (assuming no leading-edge suction for the separated flow) is then derived as:

$$C_L = \sum_{i=1}^{n} \Delta F_i \cos\alpha_i \Big/ \frac{1}{2}\rho U^2 s \tag{8}$$

$$C_D = \sum_{i=1}^{n} \Delta F_i \sin\alpha_i \Big/ \frac{1}{2}\rho U^2 s \tag{9}$$

where s is the wing area.

Once the above-described calculation is completed, a time increment Δt is added and the wing is advanced to its new location. Then a vortex ring is shed both at the trailing- and leading-edge panels, as shown in Fig. 1. The strength of the latest shed-vortex ring is set equal to the bound-vortex strength at the various time step. The schematic shedding procedure shown in Fig. 1 is actually performed over the whole wing and the number of panels used was considerably more (15-55) than indicated in the drawing. As the wake-shedding process is completed, the bound vorticity is calculated by Eq. (3), the wake rollup performed with Eq. (5), and the forces acting are indicated by Eqs. (8) and (9). The preceding calculational scheme is then repeated for the additional time intervals.

Results

The development of the nonsteady model has been carried out in several steps to ensure that the model complied with the physical phenomena. In the first stage the behavior of delta wings, which were suddenly set into motion, was investigated. The investigation was done for both small angles of attack, where the flow is attached, and for high angles of attack, where leading-edge separation occurs. Delta wings oscillating with small-amplitude harmonic oscillation were then treated. The third part included combined harmonic oscillations and plunging motions. This combination enabled the distinction between the α and q effects. The last part consisted of the prediction of step function in the angle-of-attack effect and the behavior of the so-called indicial function.

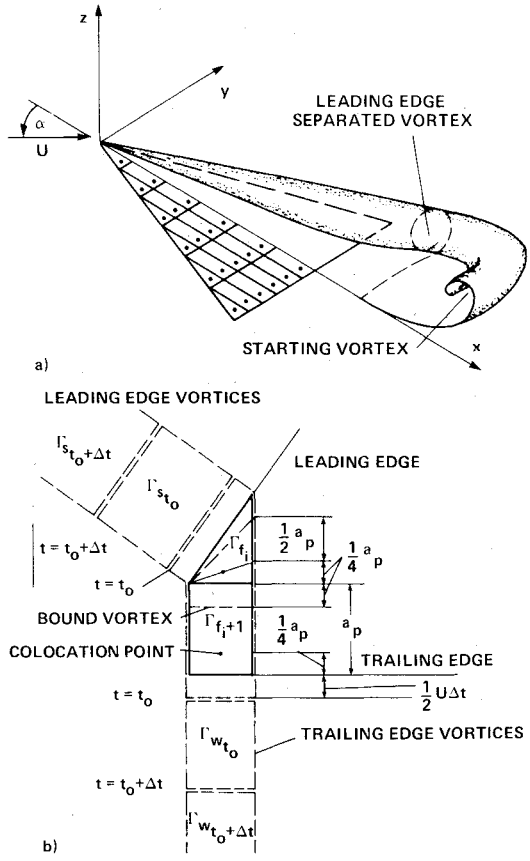

Fig. 1 Schematic of vortex-lattice method and panel geometry.

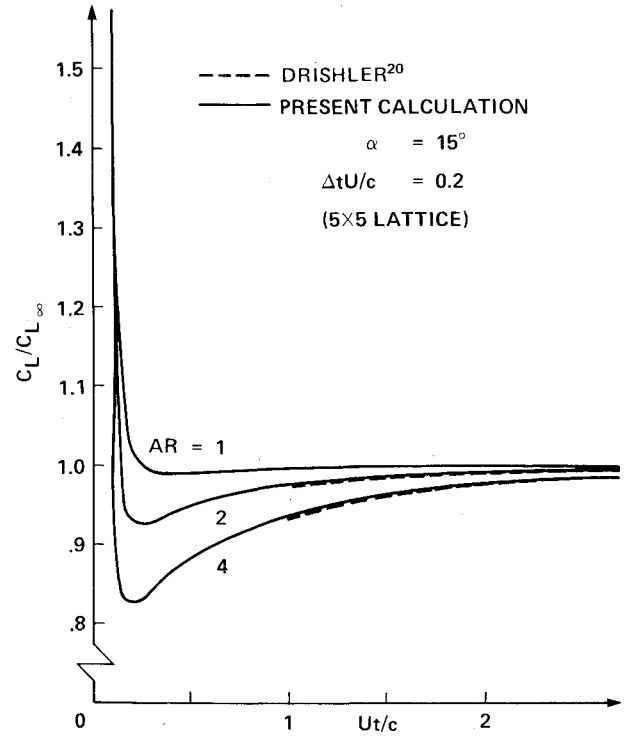

Fig. 2 Transient lift of a delta wing that was suddenly set into motion (without leading-edge separation).

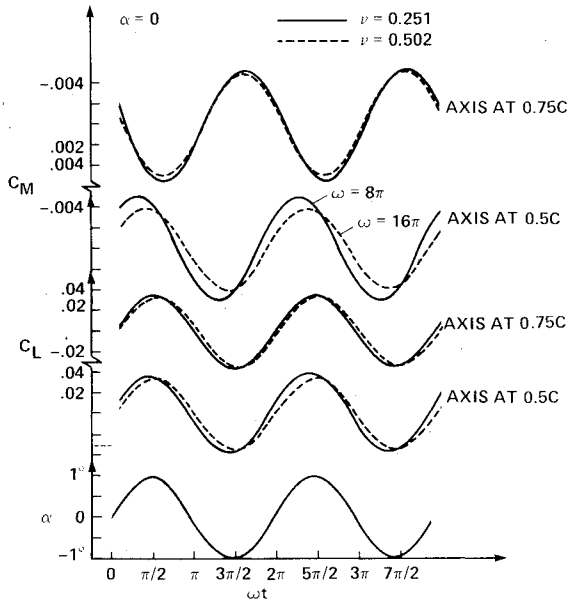

Fig. 3a Variation of the lift and moment coefficient with the oscillating angle θ.

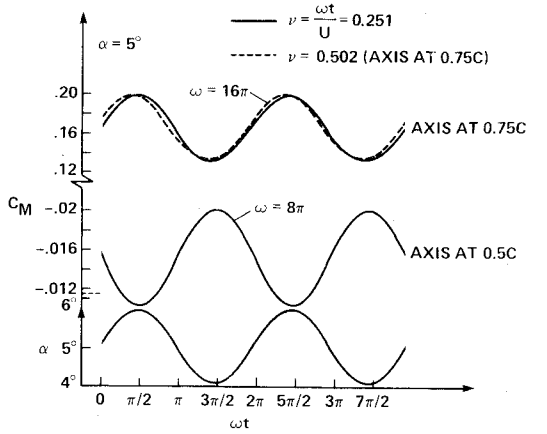

Fig. 3b Variation of the moment coefficient with the oscillating angle θ; $\alpha = 5$-deg axis location at 0.5 and 0.75 chord.

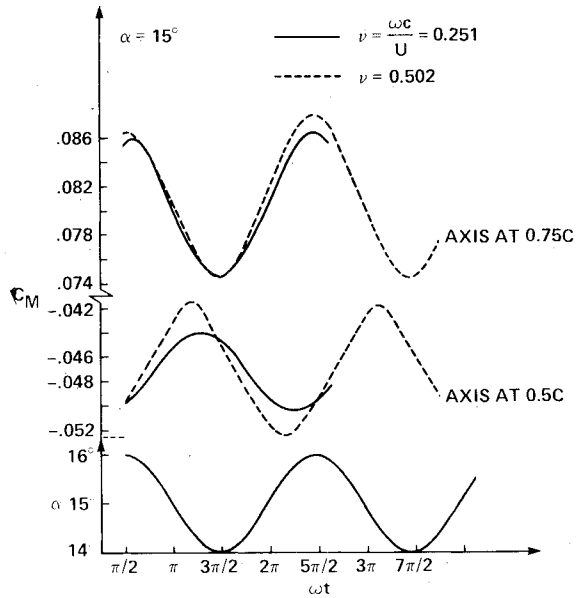

Fig. 3c Variation of the moment coefficient with the oscillating angle θ; $\alpha = 15$-deg axis location at 0.5 and 0.75 chord.

Impulsively Started Wings

The results of this investigation were reported in Ref. 16. A typical behavior is shown in Fig. 2. The results for low angle of attack agreed well with the calculations of Drishler.[20] The steady-state results for high and low angles of attack agreed well with both the iterative steady vortex-lattice method and experimental data.

Delta Wings in Small Oscillations

Intensive experimental work on delta wings in forced oscillations in subsonic flow has been carried out by Woodgate.[21] A semi-empirical work based on the same wing is suggested by Ericsson and Reding.[22] The present calculations were developed to compute the same model. The nomenclature of Ref. 21 is used here to enable easy comparison. The oscillations are of small magnitude (1 deg) and simple harmonic in the pitch plane. The oscillatory angle θ is defined by

$$\theta = \theta_0 \sin\omega t \tag{10}$$

where $\theta_0 = 1$ deg and ω is the oscillation frequency. The following expression describes the pitching moment.

$$M = M(\alpha) + [M_\theta \sin\omega t + \omega M_{\dot\theta} \cos\omega t]\theta_0 \tag{11}$$

where $M(\alpha)$ is the component of the moment due to the mean angle of attack. The moment coefficients are defined as follows.

$$m_\theta = M_\theta / \tfrac{1}{2}\rho U^2 sc \qquad m_{\dot\theta} = M_{\dot\theta} / \tfrac{1}{2}\rho U^2 sc \tag{12}$$

It follows, then, that the moment coefficient is given by

$$C_m = C_{m(\alpha)} + [m_\theta \sin\omega t + \nu m_{\dot\theta} \cos\omega t]\theta_0 \tag{13}$$

where $\nu = \omega \bar{c}/U$ is the reduced frequency.

The axis of the pitch oscillations was located at either 0.5 or 0.75 of the root chord. The mean angle of attack varied between 0, 5, and 15 deg. The freestream velocity and the oscillation frequency could be chosen arbitrarily to produce the desired reduced frequency. The reduced frequencies chosen where $\nu = 0.251$ and 0.502 in several different oscillation frequencies. The results of these runs are shown in Fig. 3 and Table 1. In Fig. 3a, the results for $\alpha = 0$ deg show that the lift is effected mainly by the momentary angle and that neither the axis location nor the reduced frequency has a significant effect. This is not the case of the moments, because the location of the axis not only decides on the sign of the moment, but also changes the phase lag between the moment and the angle of attack. Another effect that can be noticed is that the reduced frequency has very little effect when the axis is located at 0.75 chord, which shows that $M_{\dot\theta}$ must be small for this location. The amplitudes of the moments in the case of $\alpha = 0$ deg are the same for both axis locations; this is not so, however, for the case of higher mean angles of attack, as shown in Figs. 3b and 3c. The effect of angle of attack is clearly demonstrated on the mean value of the moment and on the amplitude of the oscillations. The results for the in-phase and out-of-phase coefficient are shown in Table 1.

In Table 1, the results obtained by the new method are compared with the experimental data of Ref. 21. The agreement is good except for the case of $\alpha = 15$ deg and the axis located at 0.75 chord. A comparison of the predicted and measured results is shown in Fig. 4 at $\alpha = 0$ and 15 deg. Several oscillation frequencies and freestream velocities were investigated; as a rule, the method is insensitive to the actual frequency if the reduced frequency is held constant. On the other hand, the program is sensitive to the initial condition of the beginning of the motions and the time step. For the high angles of attack a relaxation period is necessary before the harmonic behavior stabilizes. The number of panels (5×5)

was enough for all purposes; in several cases, a higher number (8×8) yielded the same results. Computer time consumed varied from linear to nonlinear cases and depended on the length of the desired time history; runs used 10-200 s on the CDC 7600.

Oscillations Combined with Plunging Motion

The combination of oscillations and plunging motion was used to simulate the two motions shown in Fig. 5. The snaking maneuver that holds the angle constant and lets q change defines the C_{M_q} component of the moment. The oscillation in plunge motion that lets the angle of attack change, while holding $q=0$ defines the $C_{M_{\dot\theta}}$ component. The capability for separating the two components helps to understand the different effects each of the two motions has on the overall longitudinal stability. A different behavior occurs for different axis locations (Fig. 6). The coefficients obtained in this manner are presented in Table 2. The agreement between these coefficients and those derived in the previous section is good. These results support the suggestion made by Tobak and Schiff[23] that the motion can be divided into several components in linear manner, even though the motion lies in the nonlinear range.

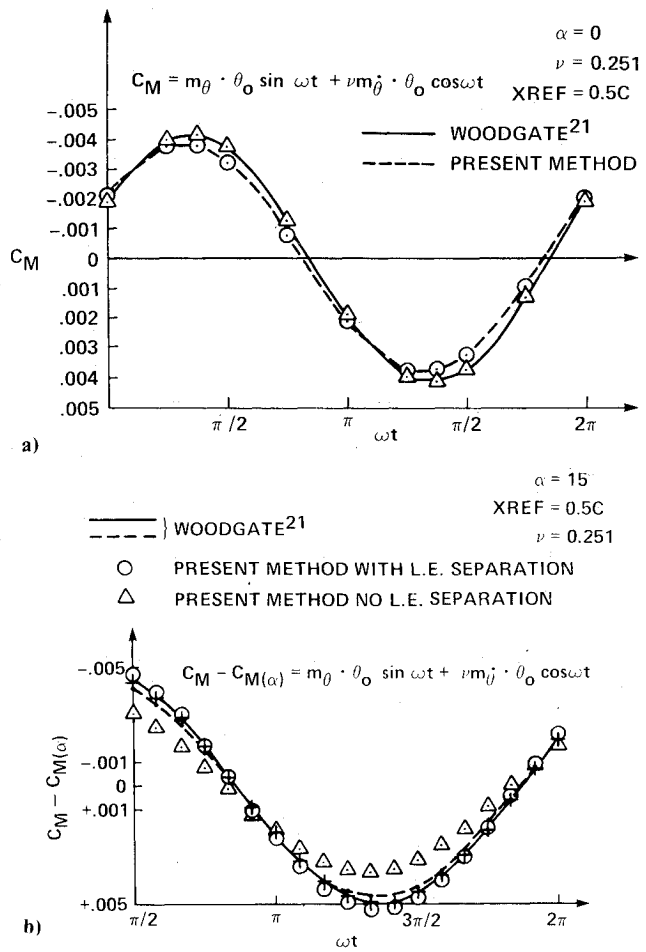

Fig. 4 Variation of nonsteady moment coefficient with oscillating angle θ ($\theta=\sin\omega t$).

Indicial Function

The work of Tobak and Schiff[23] suggests that with certain assumptions the dynamic response of a wing could be analyzed by the use of the indicial function. If a step function is applied to the angle of attack, the behavior of the pitching moment following the step would depend on the stability derivative. Following Ref. 23, a deficiency function is introduced:

$$F(t,\alpha,q)=C_m(t=\infty,\alpha,q)-C_m(t,\alpha,q) \tag{14}$$

For slowly varying harmonic oscillations, it is shown that for time periods sufficiently large, the following equation applies:

$$C_{M_{\dot\theta}}=-\frac{U}{\ell}\int_0^{t_a}F(\tau,\alpha,q=0)\,d\tau \tag{15}$$

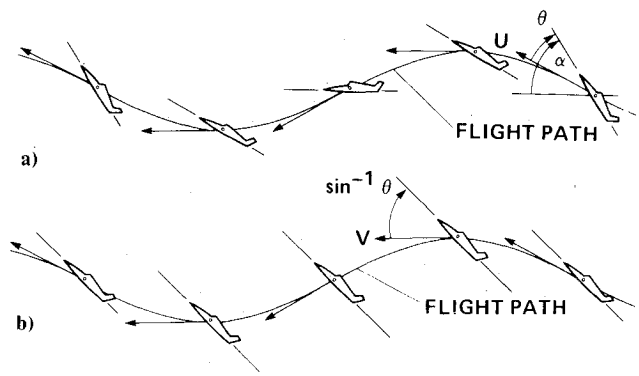

Fig. 5 Separation of oscillation motion into the q and $\dot\theta$ effects. a) Snaking maneuver with θ held fixed; definitive motions for the evaluation of C_{M_q}; b) oscillations in plunge motion defining $C_{M_{\dot\theta}}$.

Table 1 Comparison of calculated and measured values of m_θ and $m_{\dot\theta}$

		$X_{ref}=\bar C=0.5C$			
		m_θ		$m_{\dot\theta}$	
α, deg	ν	Experimental	Computed	Experimental	Computed
0	0.188	−0.213	−0.1873	−0.449	−0.486
	0.251	−0.212	−0.1833	−0.440	−0.478
	0.502	−0.220	−0.1776	−0.439	−0.467
5	0.188	−0.268	−0.186	−0.501	−0.498
	0.251	−0.266	−0.190	−0.498	−0.496
15	0.251	−0.242	−0.2716	−0.467	−0.525

		$X_{ref}=1.5\,\bar C=0.75\,C$			
			m_θ		$m_{\dot\theta}$,
α, deg	γ	m_θ	Computed	$m_{\dot\theta}$	Computed
0	0.181	0.257	0.292	−0.075	—
	0.251	0.244	0.292	−0.066	−0.068
	0.502	0.272	0.303	−0.074	−0.074
5	0.251	0.251	0.288	−0.080	−0.08
15	0.251	0.487	0.338	−0.300	−0.052

where t_a is the time needed for the deficiency function to vanish ($t > t_a$), U the freestream velocity, and ℓ a length factor. The prediction of the nonsteady vortex-lattice method as to the behavior following a step change in the angle of attack is very sensitive to the time step used in the calculation. This procedure has not been thoroughly investigated, but several results similar to those shown in Fig. 7 demonstrate the ability of the nonsteady code to react even to a step function in the time history. The results obtained in this way are shown in Table 2 and are similar to those obtained by the oscillation and plunging motions.

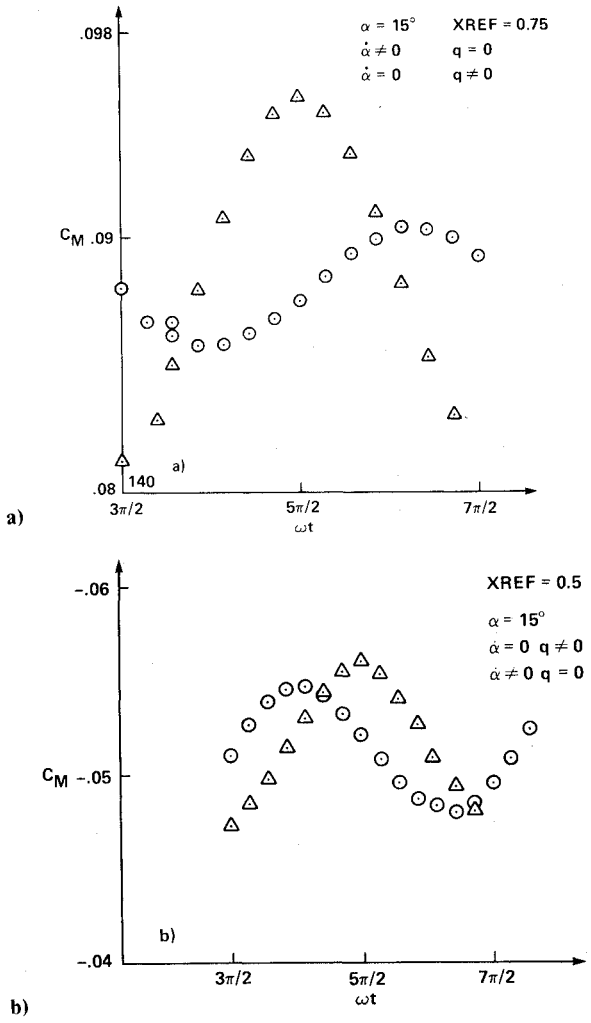

a)

b)

Fig. 6 Variation of $C_{M_{\dot\theta}}$ and C_{M_q} with the oscillating angle θ ($\theta = \sin\omega t$).

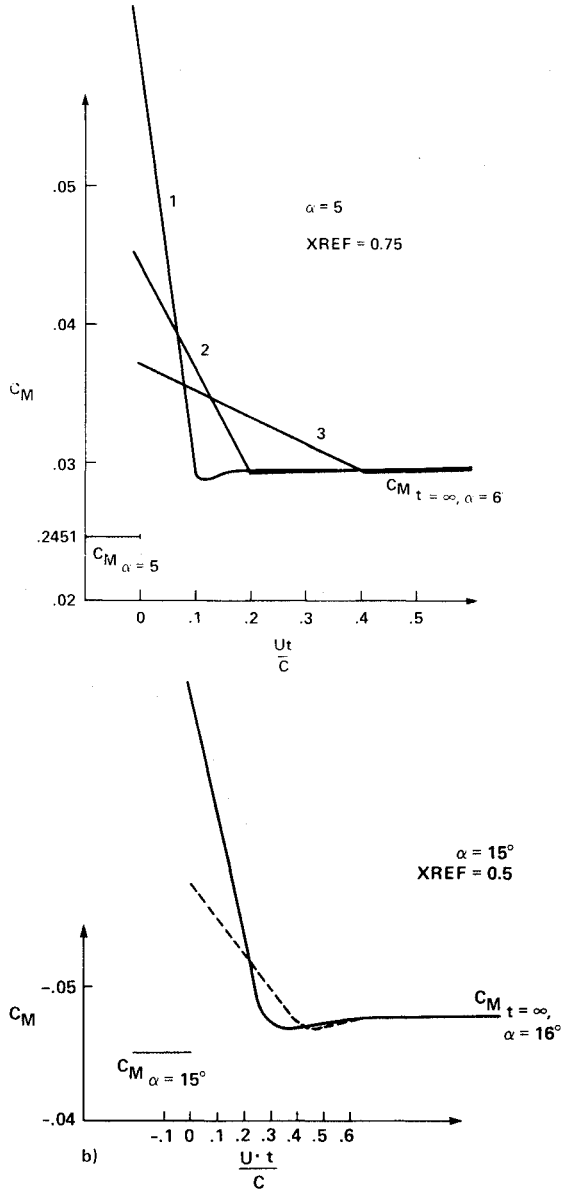

a)

b)

Fig. 7 Time response of the moment coefficient to a 1-deg step in the angle of attack for various time step calculations.

Table 2 Comparison of C_{M_θ} and $C_{M_{\dot\theta}}$ calculated by separate and combined motions

			Calculated		Measured	
	C_{M_q}	$C_{M_{\dot\theta}}$	C_{M_θ}	$C_{M_q}+C_{M_{\dot\theta}}$	C_{M_θ}	$C_{M_{\dot\theta}}+C_{M_q}$
			$\alpha = 0$ deg			
$X_{ref}=0.5$						
$\nu=0.251$	−0.376155	−0.085496	−0.189076	−0.4616	−0.1833	−0.478
$\nu=0.5$	−0.382352	−0.088455	−0.195379	−0.4708	−0.1776	−0.467
$X_{ref}=0.75$						
$\nu=0.5$	−0.145918	+0.077611	0.288	−0.0683	0.303	−0.074
$\nu=0.251$	−0.14134	+0.07637	0.2715	−0.06497	0.292	−0.068
			$\alpha = 15$ deg			
$X_{ref}=0.5$						
$\nu=0.251$	−0.38718	−0.137909	−0.27158	−0.525089	−0.514026	−0.29937
$X_{ref}=0.75$						
$\nu=0.251$	−0.25758	0.199456	0.415394	−0.058127	0.338045	−0.051289

Concluding Remarks

The nonsteady vortex-lattice method is shown to be a useful tool for predicting the dynamic stability derivatives. The prediction of the damping in pitch is obtained in several ways. It can be separated into the α and q components, and there is good agreement between the predicted results and experimental data. At present, calculations are restricted to symmetrical wings and motions, but the method can be extended to include lateral motions, lateral stability derivatives, and cross coupling of lateral and longitudinal motions. Two intermediate goals for this extension are better simulation of the leading-edge separation and, possibly, the development of a potential way of modeling the vortex breakdown.

References

[1]Thomas, H.H.B.M., "State of the Art of Estimations of Derivatives," AGARD Rept. 339, 1961.

[2]Ellison, D. E. and Hoak, D. E., "Stability Derivative Estimations at Subsonic Speeds," *International Congress on Subsonic Aeronautics*, N.Y. Academy of Sciences, 1968, pp. 367-396.

[3]Schneider, C. P., "Analytical Determination of Dynamic Stability Parameters," AGARD LSP-114, 1981, p. 12.

[4]Garner, H. C., "Multhopp's Subsonic Lifting-Surface Theory of Wings in Slow Pitching Oscillations," ARC R&M 2885, 1952.

[5]Lehrian, D. E. and Garner, H. C., "Theoretial Calculation of Generalized Forces and Load Distribution on Wings Oscillating at General Frequency in Subsonic Stream," ARC R&M 3710, 1971.

[6]Morino, L., "A General Theory of Unsteady Compressible Potential Aerodynmaic," NASA CR-2464, 1974.

[7]Kalman, T. P., Rodden, W. P., and Giesing, J. P., "Application of the Doublet-Lattice Method to Non-Planar Configurations in Subsonic Flow," AIAA Paper 70-539, 1970.

[8]Dusto, A. R. and Epton, M. E., "An Advanced Panel Method for Analysis of Arbitrary Configurations in Unsteady Subsonic Flow," NASA CR-152323, 1980.

[9]Atta, E. H., Kandil, O. A., Mook, D., T., and Nayfeh, A. H., "Unsteady Aerodynamic Loads on Arbitrary Wings Including Wing-Tip and Leading-Edge Separation," AIAA Paper 77-156, 1977.

[10]Kandil, O. A., Atta, E. H., and Nayfeh, A. H., "Three-Dimensional Steady and Unsteady Asymmetric Flow Past Wings of Arbitrary Planforms," AGARD CP-227, Sept. 1977.

[11]Kandil, O. A., "State of Art of Nonlinear Discrete-Vortex Method for Steady and Unsteady Angle of Attack Aerodynamics," AGARD CP-247, 1978.

[12]Djojodihardjo, R. H. and Widnall, S. E., "A Numerical Method for the Calculation of Nonlinear Unsteady Lifting Potential Flow Problems," *AIAA Journal*, Vol. 7, 1969, pp. 2001-2009.

[13]Belotserkovskii, S. M., "Study of the Unsteady Aerodynamics of Lifting Surfaces Using the Comptuer," *Annual Review of Fluid Mechanics*, 1977, pp. 469-494.

[14]Summa, J. M., "A Numerical Method for the Exact Calculation of Airloads Associated with Impulsively Started Wings," AIAA Paper 77-002, 1977.

[15]Rom, J., Almosnino, D., and Zorea, C., "Calculation of the Nonlinear Aerodynamic Coefficients of Wings of Various Slopes and Their Wakes, Including Canard Configurations," *Proceedings of the 11th Congress of ICAS*, Lisbon, Portugal, Sept. 1978, pp. 333-344.

[16]Levin, D. and Katz, J., 'A Vortex-Lattice Method for the Calculation of the Nonsteady Separated Flow over Delta Wings," AIAA Paper 80-1803, 1980.

[17]Katz, J. and Weihs, D., "Large Amplitude Unsteady Motion of Flexible Slender Propulser," *Journal of Fluid Mechanics*, Vol. 90, 1979, pp. 713-723.

[18]Robinson, A. and Laurman, J. A, *Wing Theory*, Cambridge University Press, Cambridge, Mass., 1956.

[19]Katz, J., "Method for Calculating Wing Loading During Maneuvering Flight Along a Three-Dimensional Curved Path," *Journal of Aircraft*, Vol. 16, 1979, pp. 739-741.

[20]Drishler, J. A., "Approximate Initial Lift Functions for Several Wings of Finite Span in Incompressible Flow as Obtained from Oscillatory Lift Coefficients," NACA TN-3639, May 1956.

[21]Woodgate, L., "Measurements of the Oscillatory Pitching Moment Derivatives on a Slender Sharp-Edged Delta Wing in Incompressible Flow," ARC R&M 3268, Part 2, July 1968.

[22]Ericsson, L. E. and Reding, J. P., "Unsteady Aerodynamics of Slender Delta Wings at Large Angle of Attack," *Journal of Aircraft*, Vol. 12, Sept. 1975, pp. 721-729.

[23]Tobak, M. and Schiff, L. B., "Aerodynamic Mathematical Modeling Basic Concepts," ARARD LSP-114, No. 1, 1981.